

# Fabrication of Photonic Integrated Circuits by DUV-induced Modification of Polymers

P. Henzi, D. G. Rabus, U. Wallrabe, J. Mohr

Forschungszentrum Karlsruhe, Institut für Mikrostrukturtechnik, D-76021 Karlsruhe, Germany

## ABSTRACT

The expansion of high capacity optical transmission techniques into price-sensitive areas such as datacom and access networks requires a major reduction in the cost of optical components. Polymer waveguides are attractive because they are very simple to process and are promising for low-cost devices. Deep UV-induced modification of the dielectric properties of polymers is a useful technique for low cost realization of integrated optical circuits for telecommunication and sensor applications. The technique presented here has several advantages with respect to common methods because only a single polymer layer is used, which serves as the substrate and waveguide as well and no further etching or development step is required. The integration of the waveguide circuits in a polymer microoptical bench offers the possibility of combining the devices with semiconductor based optical circuits and also achieve easy fiber-chip coupling. In this work, preliminary results of Y-junctions, directional couplers, multimode interference (MMI) couplers will be given.

Keywords: polymer, waveguide, DUV lithography, telecommunication, photonic integrated circuit

## 1. INTRODUCTION

All-optical networks provide unique opportunities for polymer waveguide devices because of their excellent mechanical and thermo-optic properties. Polymer materials and components have been viewed as a viable solution for metropolitan and local area networks where high volume and low cost components are needed. Polymeric optical waveguides have been fabricated by various techniques such as reactive ion etching<sup>1,2</sup>, photolocking<sup>3-5</sup>, laser direct-writing, electron-beam direct writing<sup>6,7</sup> and replication techniques like embossing, casting or injection moulding or hot embossing<sup>8,9</sup>. An alternative approach is the direct UV-induced modification of the dielectric properties of polymers. It was first reported by Tomlinson et al.<sup>13</sup> that polymethylmethacrylate exhibits a significant increase in the refractive index after irradiation with DUV light. Furthermore it has been shown that optical waveguides can be created in polymethylmethacrylate homopolymers through application of ionizing radiation, such as ion<sup>14</sup> and deep ultraviolet radiation<sup>15-19</sup>. In this paper, we present our recent progress on the design and development of UV-induced single mode waveguides in methylmethacrylate polymers. By systematic analysis of process parameters using basic waveguide components, the feasibilities and limits of this approach are given.

## 2. EXPERIMENTAL

The structuring of waveguides was carried out by conventional photolithographic technique using a quartz/chromium mask as sketched in Fig. 1. Thereby the refractive index of the polymer which is UV-exposed increases but that of the unexposed region does not increase. Because only a thin surface layer of a view micrometer is modified by the DUV-light, only a single polymer layer is required, which serves as the substrate and waveguide as well. The use of a single polymer substrate avoids the large mismatch of coefficients of thermal expansion (CTE) between polymeric and inorganic materials, which leads to birefringence in the polymer layers and results in temperature sensitive devices. Thus athermal and polarization insensitive polymer devices can be fabricated by employing a single substrate with a coefficient of thermal expansion matching that of the modified surface waveguide layer due to only marginal structural modification.

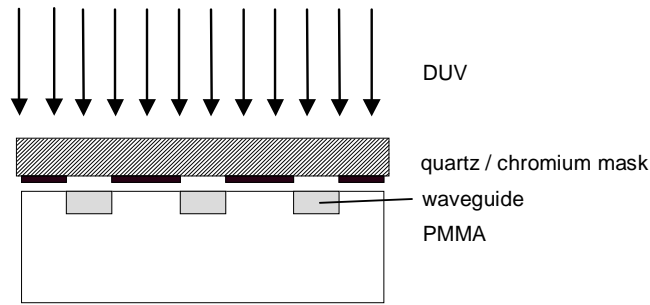


**Fig. 1:** Scheme of waveguide fabrication by a quartz /chromium mask.

For waveguide fabrication optimisation we studied the dependence of photochemistry under different environmental condition (air, vacuum or inert gas) and by changing the primary methylmethacrylate polymer properties such as molecular weight and copolymer composition. The devices were analysed using various optical characterization methods such as m-line-spectroscopy, near-field measurements, or cut-back method. For material investigation UV-VIS-spectroscopy, IR-spectroscopy, differential scanning calorimetry (DSC) were used. Details of the processing and characterization have been described elsewhere<sup>10</sup>. The material used here was Hesa@Glas a homopolymer from Notz-Plastic. It can be shown that the dominating photochemical reactions are independent of the material used. During photolysis in ambient air, photooxidation products can be detected by means of FTIR-spectroscopy. Spectral attenuation measurements of straight waveguides in the range of 1100 nm-1700 nm show different losses for waveguides exposed under air compared to those exposed in vacuum indicating the influence of vibrational overtones from R-OH photo oxidation products, which increase only the absorption in the third optical window at 1550 nm. The second optical window at 1310 nm remains unaffected (see Fig. 2 left). For our best process parameters the attenuation of the waveguides at 1550 nm is found to be 1 dB/cm for fabrication under vacuum compared to 1.7 dB/cm for waveguides processed under air (see Fig. 2 right). All waveguides are polarization independent and show typical coupling loss to a single mode fiber of 0.5 dB/facet. Furthermore first result show that the waveguides can sustain temperatures between 0°C to 85°C under continues operation.

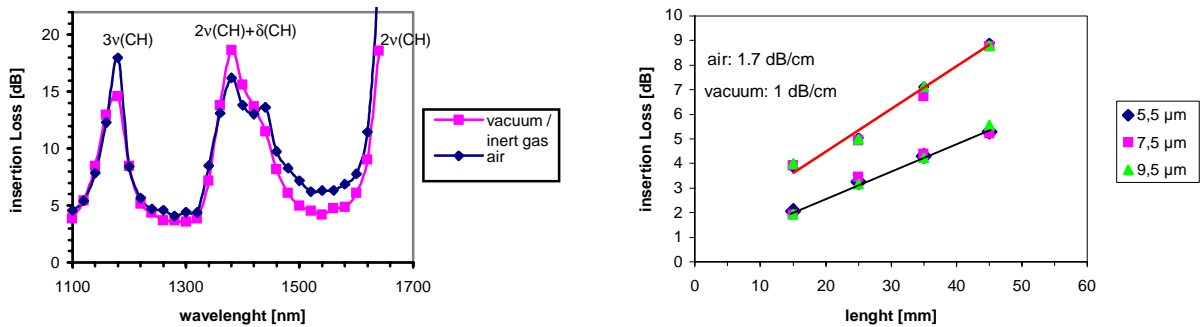


**Fig. 2:** Spectral insertion loss of 25 mm long straight waveguides (left). Insertion loss of straight waveguides in dependence of length and width (right).

### 3. RESULTS

All basic components like strips, y-branches, directional couplers, Mach-Zehnder-interferometers are modeled using BeamProp., a commercial beam propagation software<sup>11</sup>. The structures were designed and fabricated for the 1.55  $\mu\text{m}$  wavelength region. The necessary refractive index distribution is derived from m-line-spectroscopy using an inverse WKB-method<sup>12</sup>. Then, based on the index distribution a three-dimensional semivectorial BPM-method calculation was carried out. For loss minimization the dependence on the width of the waveguide, bending radius, branching angle and refractive index distribution due to fabrication process parameters was investigated.

#### 3.1. Symmetrical Splitter

Symmetrical 1 x 2 splitters with different angle were fabricated by combining pairs of s-bend structures. S-bends structures were composed of two identical arcs. For s-bends with radii of curvature greater than 6 mm no additional propagation loss was observed. After waveguide fabrication the polymer wafers are separated by a wafer saw into waveguide chips of 25 mm width. No further polishing of the end faces was carried out. In Fig. 3 a light microscope photograph of a part of a 1 x 2 splitter is shown. On the right side a typical near field pattern of the end face of a 1 x 2 splitter is shown. An uniform splitting of the light into the two branches and no scattered light between the waveguides could be observed.

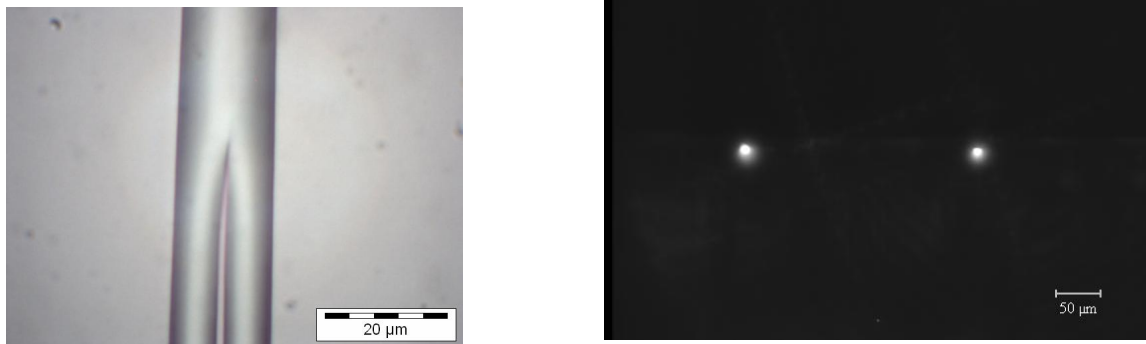


**Fig. 3:** LM-photograph of a symmetrical 1 x 2 splitters (left). Near field photograph of the 1 x 2 splitter end face (right).

Simulated insertion loss in dependence of branching angle show no significant loss for angles smaller than 2°. Splitters were fabricated by varying the branching angle from 1° to 2.5°. For small angles the measured curves exhibit a higher loss due to processing imperfections caused by limited photolithographic resolution at the Y-junctions. As an example the spectral insertion loss characteristic of the two output ports of a 1 x 2 splitter with branching angle of 1.75° are depicted in Fig. 4. For comparison the spectral insertion loss of a 25 mm straight waveguide is shown, too. The coupler shows an insertion loss of 7 dB at 1550 nm, including 3 dB of functional splitting loss. Since a straight waveguide of length 25 mm has an insertion loss of 3.5 dB, the additional loss due to splitting is in the range of 0.5 dB. The uniformity of the output ports is in the measurement accuracy of 0.1 dB.

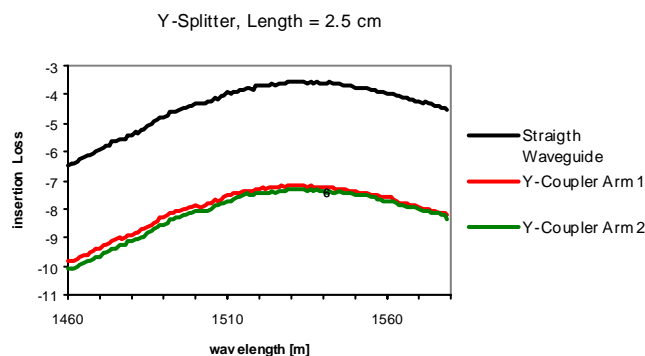


**Fig. 4:** Wavelength dependent insertion loss of a symmetric Y-coupler.

### 3.2. Codirectional Coupler

Another important device, which we use to characterize our process parameters and investigate the limits of our waveguide fabrication approach, is a 2 x 2 codirectional coupler. This type of coupler can be used for equal splitting of the power independent from the input channel in the whole wavelength region, as well as to realize splitting ratio other than 3 dB. The design of the directional coupler is very important. Our design tools were used to design a symmetric (identical waveguide geometries), wavelength flattened coupler with low excess loss. The separation between the waveguides in the coupling region is the critical element regarding the fabrication. The resolution of the photolithography defines the minimum coupling gap, which is about 1  $\mu\text{m}$  in our case. Since the structures are weak guiding, the coupling gap could be chosen in the range of 1 to 5  $\mu\text{m}$ .

A light microscope photograph of the coupling section is shown in Fig. 5. The measured result of a codirectional coupler with a coupling gap of 3  $\mu\text{m}$  and different coupling length are shown on the right side. The intensity at both output ports is normalized to the sum of the output intensities. The couplers losses are less than 10%. The measured values confirm the simulation quiet well.

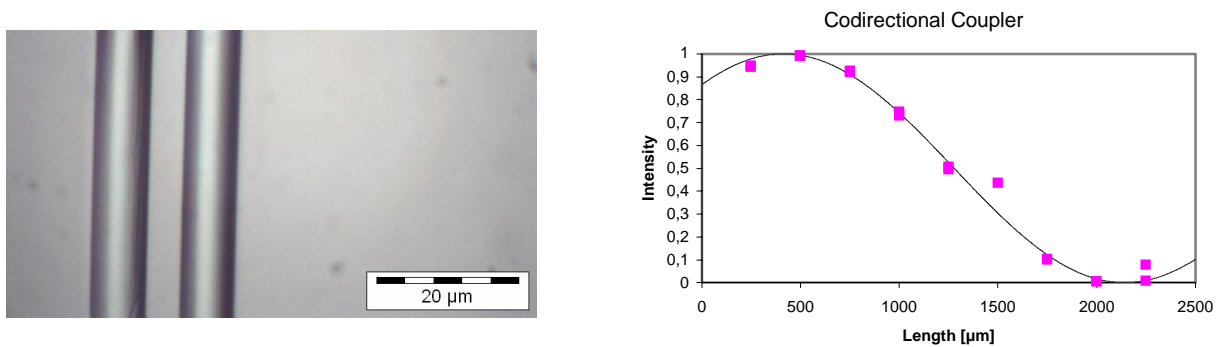


**Fig. 5:** LM photograph of the coupling section of a codirectional coupler (left). Splitting ratio, couplergap 3  $\mu\text{m}$  (right).

### 3.3. Multimode-interference-coupler (MMI)

Another basic component which is implemented for a variety of optical signal processing and routing functions is a multimode-interference coupler (MMI). In Fig. 6 a 2 x 2 MMI coupler is depicted. The coupler consists of a broad centre waveguide which supports several modes depending on the width of the waveguide.

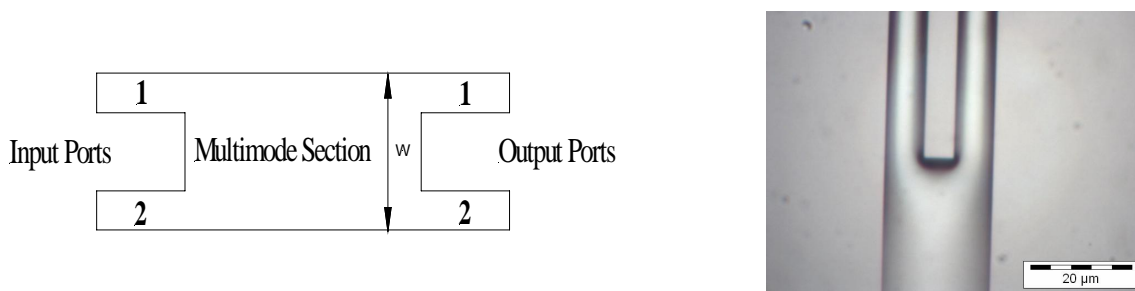


**Fig. 6:** Scheme of a 2 x 2 MMI coupler (left). LM-photographs of the input Region of a 3 dB Multimode Interference (MMI) Coupler (right).

These multimode interference devices offer important advantages such as compact size, low imbalance and crosstalk<sup>20</sup>. In comparison to codirectional couplers the main advantage is the fabrication tolerance. Most of these devices have so far been fabricated in high index contrast materials like InP. For high index contrast materials this type of waveguide has nearly an ideal mode spectrum which ensures a proper self-image. To date there has only been limited application of polymer materials for MMI devices. An important limitation on broader use is that typical polymer waveguide have low index contrast, therefore the modes are so weakly confined that the eigenmode spectrum deviates greatly from the

ideally required mode spectrum for self-imaging<sup>21</sup>. Thus the imaging quality is significantly degraded, exhibiting an increased loss and imbalance. However, our simulation show at the best image point tolerable loss and imbalance which justify to fabricate a weak guiding MMI coupler. The designed MMI coupler has a width of 27  $\mu\text{m}$ . As can be seen in Fig. 7 there are 4 modes which are supported in the broader multimode section. The mode solving is done via BPM using the correlation method. The multimode section should support more than three modes to assure an appropriate interference signal. The interference pattern of the 4 modes in transmission direction is shown in Fig. 7 on the right side. In the range between 1650-1950  $\mu\text{m}$ , the intensity of the MMI is divided equally at both of the output ports.

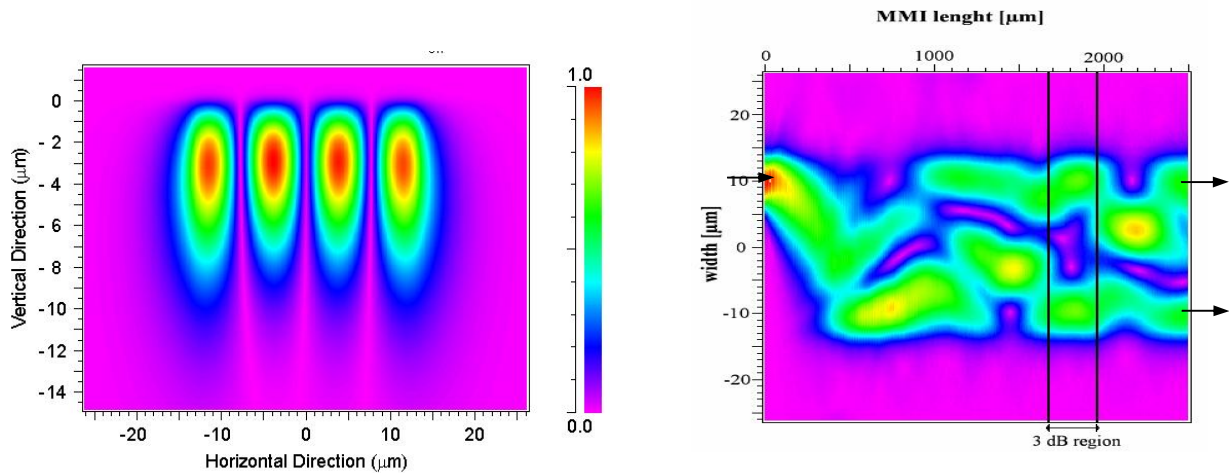


**Fig. 7:** Simulated modeprofile of a MMI coupler, TE polarization (left). Simulation of the interference pattern in transmission direction, TE polarization (right).

Fig. 8 illustrates the calculated output coupling intensities as a function of the length of the MMI region. The best image point in terms of 3 dB splitting ratio, low loss and imbalance is around 1800  $\mu\text{m}$ . The device has a length tolerance of  $\pm 150 \mu\text{m}$  for a 5 % imbalance in splitting ratio. The MMI is nearly polarization independent with respect to the 3 dB point. This is an advantage compared to codirectional couplers. The measured results of the MMI coupler as a function of the length of the MMI region around the 3-dB imaging point are shown on the right side. The intensities of both outputs of the MMI coupler have been added and normalized. These first results show that MMI devices can be realized in polymers. Further design and fabrication improvements will increase the device performance.

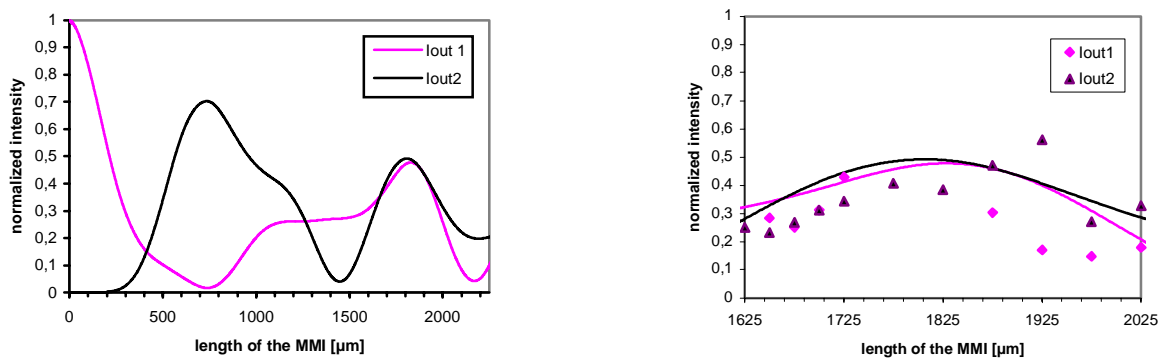


**Fig. 8:** Simulation of the intensities at the output ports of a MMI with width of 27  $\mu\text{m}$  in the multimode region (left). Measured intensities at the output ports of the MMI coupler at different lengths (right).

### 3.4. Waveguide fabrication pre-patterning by hot embossing

Since fibre alignment and assembly are serious difficulties and cost factors in a mass production of integrated optical devices, an alternative process variant was worked out, which allows a passive alignment and assembly. The approach uses the LIGA-technique in a first step to pre-emboss the polymer substrate. Details of the process are described elsewhere<sup>10</sup> Fig. 9 shows a side view of the pre-embossed substrate for waveguide fabrication. At this stage the embossed ridge or groove structure serves as the masking structure for the ensuing flood exposure. If the penetration depth of the evanescent field of these waveguides is smaller than the distance between them and the planar waveguides at the surface, no light can couple from one waveguide into the other waveguides. Either the ridge or groove waveguides can be used as stripe waveguides. Since the effect of UV-induced material modification typically produces refraction index differences that are small and causes these guides to be very lossy in bends, ridge waveguides are preferred for strong guiding application, for weak guiding application the groove structure is used. Additionally, waveguides and fiber alignment grooves can be produced in one fabrication step. Furthermore it's possible to integrate functional sidewalls like mirrors or gratings. The fabrication of the microoptical bench and the waveguides in the same process step assures very good alignment accuracy and guarantees a low cost passive fiber-chip coupling and assembly. The approach presented here provides the opportunity to have a mass fabrication process using replication technologies like hot embossing or injection moulding.

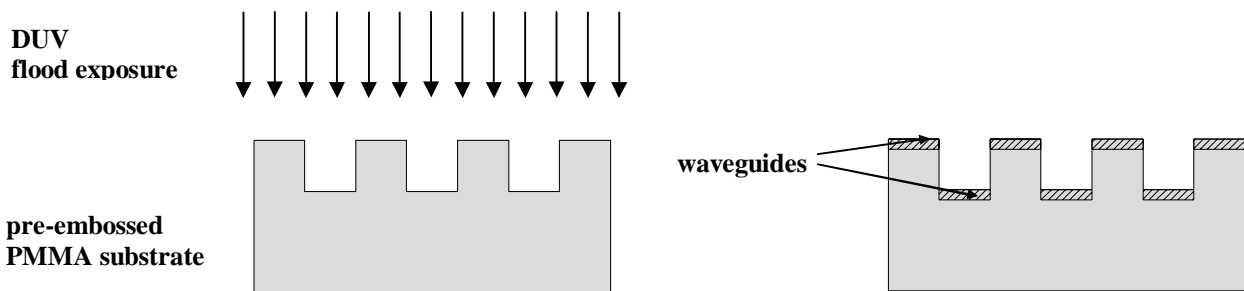


**Fig. 9:** Side view scheme of waveguide fabrication with pre-embossed polymer substrates.

Fig. 10 show SEM photographs of pre-embossed substrates with fiber alignment structures and groove or ridge waveguides. Elastic ripples in the side walls of the fiber fixing structures, facilitate fiber insertion. They also make the alignment insensitive to variations in fiber diameter.

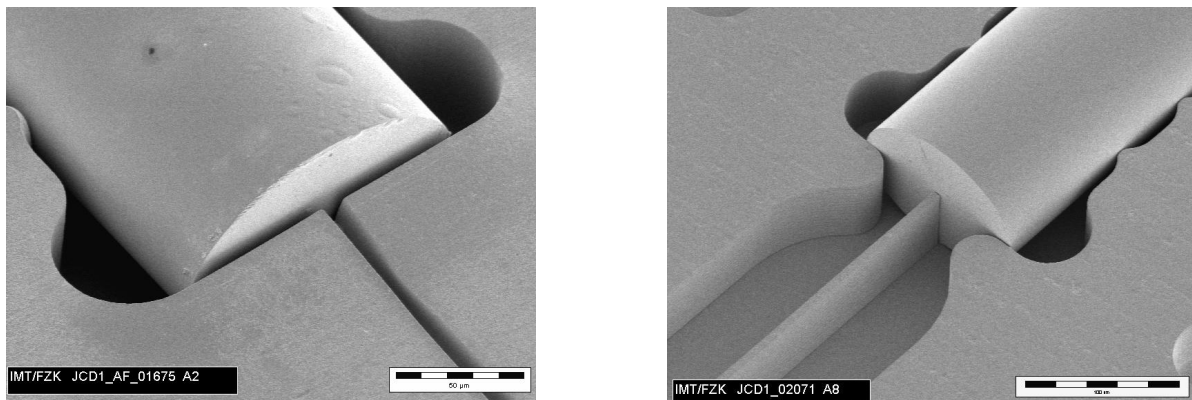


**Fig. 10:** Pre-embossed substrate in PMMA containing waveguide and passive fiber alignment structures.

The proof of principle of the fabrication of waveguides structured by masking with pre-embossed polymer substrates and following flood exposure is demonstrated in Fig. 11, which shows a near field photograph of the facet of a groove (left) and a ridge waveguide (right). Also an intense single mode profile is found. For this, the fibers are inserted into the alignment structures. Since the gap at the front face of the waveguide is 2 µm smaller than the fiber diameter, the

fibers are clamped gently by the alignment structures, thus allowing easy handling during the on-going characterization. The attenuation of the waveguides at 1550 nm is found to be 4 dB/cm. This is mainly due because of a roughness of about 100 nm rms of the top surface of the waveguides due to end-milling imperfections of the two level LIGA copper substrate which leads to increased scattering losses compared to the waveguides fabricated by conventional lithography. This problem can easily be solved by polishing the substrate.

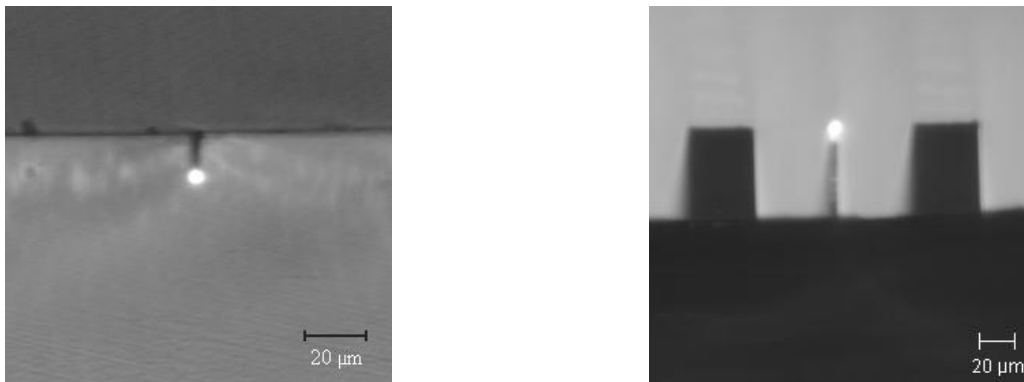


**Fig. 11:** Near field photograph of waveguides realized by masking by a pre-embossing substrate and ensuing flood exposure. Pre-embossed groove (left) and pre-embossed ridge waveguide (left).

#### 4. CONCLUSION

We have introduced a process of UV-induced fabrication of single mode waveguides in methacrylate polymers that offers the feature of a simple waveguide fabrication process. Y-Couplers, codirectional couplers and 3 dB MMI couplers have been fabricated to demonstrate the capability of this technology. Furthermore patterning of waveguides by masking with pre-embossed polymer substrates and following flood exposure was demonstrated. The approach using LIGA-techniques provide the opportunity to integrate the waveguides in a micro-optical bench. For demonstration, waveguides with passive fibre alignment structures have been successfully fabricated. The approach presented here provides the opportunities to have a mass fabrication process using replication technologies of a microoptical bench with integrated singlemode waveguides. The fabrication of the microoptical bench and the waveguides in the same process step insures very good alignment accuracy and guarantees a low cost passive coupling and assembly. Beside applications in telecommunication the fabrication process opens up new applications in the field of sensor technology. In order to protect the waveguides from moisture, dust or other physical damage, and to improve the long term stability of the polymer device, in future the addition of an upper cladding layer is essential.

#### REFERENCES

1. J. Kobayashi, T. Matsuura, S. Sasaki: *Singlemode optical waveguides fabricated from fluorinated polyimides*; Appl. Optics, 37, pp. 1032-1037, 1974
2. N. Keil; HH. Yao; Zawadzki, et al.: *Athermal all-polymer arrayed-waveguide grating multiplexer*; Electronics Letters, 37 (9): pp. 579-58, 2001
3. E.A. Chandross, C. A. Pryde, W. J. Tomlinson et al.: *Photolocking - A new technique for fabricating optical waveguide circuit*; Appl. Phys. Letter 24, pp. 72-74, 1974
4. B. L. Boot: *Polymers for optical interconnects*. Proc. OFC 95, San Diego, Californien, pp. 252-275, 1995
5. N. Keil, H.H. Yao, C. Zawadzki: *2 x 2 digital optical switch realized by polymer waveguide technology* Electron. Lett 32, pp. 1470-1471, 1996
6. N. Keil, B. Strelbel et al.: *Optical polymer waveguide devices and their applications to integrated optics and optical signal processing*. SPIE-The International Society for Optical Engineering, Vol. 1774, Nonconducting Photopolymers and Applications: pp.130-141, 1992
7. H. Einsiedel, S. Mittler-Neher: *Scanning beam deflection imaging with and without contrast inversion on polymers for integrated optical application*. Thin solid films, 288: pp. 243-247, 1996

8. H. Kragl, R. Hohmann, C. Marheine et al.: *Low cost monomode, integrated optics polymeric components with passive fiber-chip coupling*; Electronics Letters, 1997, Vol. 33, No. 24, pp. 2036-2037
9. HD Bauer, W. Ehrfeld; M. Harder et al.: *Polymer waveguide devices with passive pigtailling: an application of LIGA technology*, Synthetic Metals, 115 (1-3): pp. 13-20, 2000
10. P. Henzi, D. G. Rabus, K. Bade et al.: *Low Cost Single Mode Waveguide Fabrication Allowing Passive Fiber Coupling using LIGA and UV flood exposure*, current conference (5454)
11. BeamProp™ Version 5; RSoft, Inc. and Columbia University
12. J. M. White, P. F. Heidrich: *Optical waveguide refractive index profiles determined from measurement of mode indices: a simple analysis*; Applied Optics Vol. 15 No. 1, pp. 151-155
13. W. J Tomlinson, I. P. Kaminow, E. A. Chandross et al.: Appl. Phys. Letters 16, 486, 1970
14. D. M Rück, S. Brunner, K. Tinscher et al.: *Production of buried waveguides in PMMA by high energy ion implantation*; Nuclear Instruments and Methods in Physics Research B, 106, pp 447-451, 1995
15. W. Hong, H-J Woo, H-W Choi et al: *Optical property modification of PMMA by ion beam implantation*; Applied surface science, 169-170, pp. 428-432, 2001
16. W. F. X. Frank et al.: *Ionizing Radiation for Fabrication of optical Waveguides in Polymers*. SPIE Critical Review Conference, Vol. 63, pp. 65-83, 1996
17. A. Schösser et al.: *Optical Components in Polymers*. SPIE Proceedings, Vol. 2540: pp.110, 1995
18. A. Schösser, W. F. X. Frank et al.: *Spectroscopic Study of Surface Effects in Polymer Waveguides Generated by Ionizing Radiation Related to Guiding Properties*. SPIE Proceedings., Vol. 2851, 1996
19. A. Schösser, W. F. X. Frank et al.: *Fiber chip coupling and refractive index profile of UV-generated waveguides in PMMA*. SPIE Proceedings, Vol. 3135: pp.144-151, 1997
20. L.B. Soldano, E.C.M. Pennings: *Optical multimode interference device based on self-imaging: Principles and application*; J. Lightwave Techol., vol. 13, pp. 615-627, 1995
21. J. Z. Huang, M. H. Hu, J. Fujita: *High-performance metal-clad multimode interference devices for low-index-contrast material systems*; Photonics Technology Letters, vol. 10, No. 4, 1998